11th International Conference on Vibration Problems
Z. Dimitrovová *et.al.* (eds.)
Lisbon, Portugal, 9–12 September 2013

QUANTITATIVE ESTIMATION OF THE INFLUENCE OF EXTERNAL VIBRATIONS ON THE MEASUREMENT ERROR OF A CORIOLIS MASS-FLOW METER

L. van de Ridder*[1], W.B.J. Hakvoort[1,2], J. van Dijk[1], J.C. Lötters[1,3], A. de Boer[1]

[1]University of Twente, P.O. Box 217, 7500AE Enschede, The Netherlands
{L.vanderidder, J.vandijk, A.deBoer}@utwente.nl

[2]DEMCON, Enschede, The Netherlands
Wouter.Hakvoort@demcon.nl

[3]Bronkhorst High-Tech B.V., Ruurlo, The Netherlands
J.C.Lotters@bronkhorst.com

Keywords: Coriolis Mass-Flow Meter, Floor vibrations, PSD, Transfer function

Abstract. *In this paper the quantitative influence of external vibrations on the measurement value of a Coriolis Mass-Flow Meter for low flows is investigated, with the eventual goal to reduce the influence of vibrations. Model results are compared with experimental results to improve the knowledge on how external vibrations affect the measurement error.*

A Coriolis Mass-Flow Meter (CMFM) is an active device based on the Coriolis force principle for direct mass-flow measurements, independent of fluid properties, with a high accuracy, range-ability and repeatability. Besides the effect of the mass-flow on the mode shape of the tube, external vibrations can introduce motions that cannot be distinguished from the Coriolis force induced motion, thus introducing a measurement error.

From a multi-axis flexible body model, the transfer function between external vibrations (e.g. floor vibrations) and the flow error, including the active filter characteristics, is derived. The floor vibrations are characterised with a PSD. Integrating the transfer function times the PSD over the whole frequency range results in an RMS flow error estimate. In an experiment predefined vibrations are applied on the casing of the CMFM (white noise spectra and VC norm spectra) and the error is determined. The experimental results corresponds with the model results.

The agreement between model and measurements implies firstly that the influence of any floor vibration spectrum on the flow error, can be estimated and secondly that the performance of different CMFM designs can be compared and optimised by shaping their respective transfer functions.

1 INTRODUCTION

A Coriolis Mass-Flow Meter (CMFM) is an active device based on the Coriolis force principle for direct mass-flow measurements, independent of fluid properties, with a high accuracy, range-ability and repeatability [1]. The basic working principle of a CMFM is as follows: a fluid conveying tube is actuated to oscillate with a low amplitude at a resonance frequency in order to minimise the amount of supplied energy. A fluid flow in the vibrating tube induces Coriolis forces, proportional to the mass-flow, which affect the tube motion and change the mode shape. Measuring the tube displacement, such that the change of its mode shape is measured, allows measuring the mass-flow.

Besides the effect of the mass-flow on the mode shape of the tube, external vibrations can introduce motions that cannot be distinguished from the Coriolis force induced motion. The external vibrations create additional components in the CMFM sensor signals [2], those additional components can introduce a measurement error. For low flows, the Coriolis force induced motion is relative small compared to external vibrations induced motions, thus CMFM's designed to be sensitive to low flows, are rather sensitive to external vibrations.

The effect of mechanical vibrations on the sensor response of a CMFM is also studied by Cheesewright [3]. The analytical study showed that external vibrations at the meter's drive frequency produces a measurement error, regardless of the flow measurement algorithm. There is no attempt made to quantify the error in any particular meter, since such an error depends on dimensions, type of actuators and sensors and the used flow measurement algorithm.

In this study the effect of floor vibrations on the measurement error is quantified using an experimentally validated model. Therefore, first a model of a CMFM is derived, using the multi-body package SPACAR [4] resulting in a linear state space representation [5]. In the modelling a tube-element [6] is used to model the interaction between flow and the tube dynamics. In a previous case a CMFM is modelled for shape optimisation [7], using the same multi-body package. Secondly, the model is extended to be able to predict the influence, with the eventual goal to find and test measures that reduce the influence of floor vibrations on an erroneous mass-flow reading.

2 MODELLING

In this section, first the system equations are derived and secondly the inputs and outputs are defined to derive the input-output relations. The result of the modelling is a state-space representation of a CMFM.

2.1 System equations

For this research a functional model of the patented design [8, 9] (see Figure 1) is used. The Finite Element (FE) model is shown in Figure 2. The model consists of a tube-window, conveying the fluid flow, which is actuated by two Lorentz actuators act_1 and act_2. The displacement of the tube-window is measured by two displacements sensors s_1 and s_2. On the casing a vector $\boldsymbol{a}_0$, consisting of three translation and three rotational floor movements, is imposed.

The linearised system equations of the FE model, with n degrees of freedom of tube deformations $\boldsymbol{q}$ and the imposed casing movements $(\boldsymbol{x}_0, \boldsymbol{v}_0 = \dot{\boldsymbol{x}}_0, \boldsymbol{a}_0 = \ddot{\boldsymbol{x}}_0)$, can be written as [5]:

$$\begin{bmatrix} \boldsymbol{M}_{11} & \boldsymbol{M}_{12} \\ \boldsymbol{M}_{21} & \boldsymbol{M}_{22} \end{bmatrix} \begin{bmatrix} \ddot{\boldsymbol{q}} \\ \boldsymbol{a}_0 \end{bmatrix} + \left[\boldsymbol{C}(\dot{\Phi})\right] \begin{bmatrix} \dot{\boldsymbol{q}} \\ \boldsymbol{v}_0 \end{bmatrix} + \left[\boldsymbol{D}\right] \begin{bmatrix} \dot{\boldsymbol{q}} \\ \boldsymbol{v}_0 \end{bmatrix} + \left[\boldsymbol{K}\right] \begin{bmatrix} \boldsymbol{q} \\ \boldsymbol{x}_0 \end{bmatrix} + \left[\boldsymbol{N}(\dot{\Phi}^2)\right] \begin{bmatrix} \boldsymbol{q} \\ \boldsymbol{x}_0 \end{bmatrix} = \begin{bmatrix} \boldsymbol{f} \\ \boldsymbol{F}_0 \end{bmatrix} \quad (1)$$

The other terms are the mass matrix $\boldsymbol{M}$, stiffness matrix $\boldsymbol{K}$, proportional damping matrix $\boldsymbol{D}$,

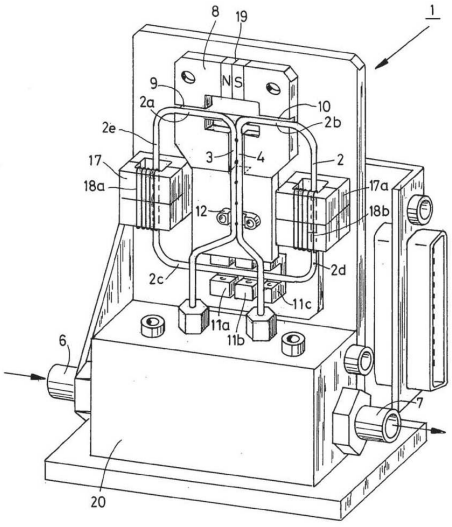

Figure 1: Coriolis Mass Flow Meter, used as a reference instrument in this study. Details on the patented design are given in [8, 9]

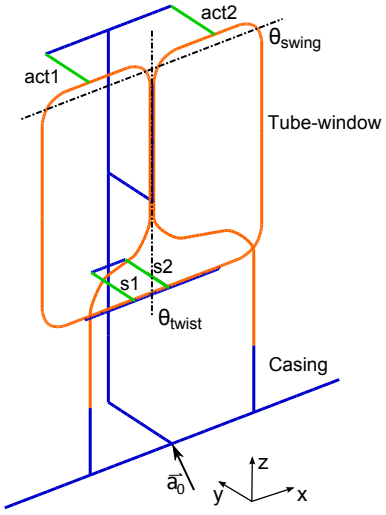

Figure 2: CMFM multi-body model, the flexible tube-window is actuated by two Lorentz actuators act_1 and act_2. The displacement are measured by two displacements sensors s_1 and s_2. On the casing a vector $\boldsymbol{a}_0$ with floor movements is imposed.

the velocity sensitive matrix $\boldsymbol{C}$, the dynamic stiffness matrix $\boldsymbol{N}$, the actuation input vector $\boldsymbol{f}$ and the reaction force $\boldsymbol{F}_0$. The matrices $\boldsymbol{C}$ and $\boldsymbol{N}$ depend on the mass-flow $\dot{\Phi}$ and are representing the forces induced by respectively the Coriolis and centrifugal acceleration of the flow. The matrices $\boldsymbol{C}$, $\boldsymbol{D}$, $\boldsymbol{K}$ and $\boldsymbol{N}$ can be divided in same parts as the mass matrix $\boldsymbol{M}$.

The matrices $\boldsymbol{C}_{12}, \boldsymbol{D}_{12}, \boldsymbol{K}_{12}, \boldsymbol{N}_{12}$ and their transposed matrices appears to be zero, for a no flow condition, due to the choice of element deformations as degrees of freedom. (E.g. $\boldsymbol{K}_{12} = \boldsymbol{0}$, because there is no coupling between the movement of the casing $\boldsymbol{x}_0$ and the internal deformations $\boldsymbol{q}$.)

The casing motion is prescribed and thus the only dynamic degrees of freedom are the tube deformations, for which the equations of motion are derived from the top row of Eq. 1:

$$\boldsymbol{M}_{11}\ddot{\boldsymbol{q}} = \boldsymbol{f} + \boldsymbol{f}_{dis} - \boldsymbol{C}_{11}\dot{\boldsymbol{q}} - \boldsymbol{D}_{11}\dot{\boldsymbol{q}} - \boldsymbol{K}_{11}\boldsymbol{q} - \boldsymbol{N}_{11}\boldsymbol{q} \tag{2}$$

including a floor disturbance force, consisting of imposed floor accelerations:

$$\boldsymbol{f}_{dis} = -\boldsymbol{M}_{12}\boldsymbol{a}_0 \tag{3}$$

The reaction forces on the floor can be derived form the lower row of Eq. 1:

$$\boldsymbol{F}_0 = \boldsymbol{M}_{21}\ddot{\boldsymbol{q}} \tag{4}$$

To reduce the degrees of freedom, a model reduction method is applied by solving the eigenvalue problem $(\boldsymbol{K}_{11} - \omega_i^2 \boldsymbol{M}_{11})\boldsymbol{v}_i = 0$, which results in natural frequencies ω_i and the corresponding eigenvector $\boldsymbol{v}_i$, the mode shape. The equations of motion are rewritten in the modal coordinates, defined as:

$$\boldsymbol{q} = \boldsymbol{V}\boldsymbol{z} \tag{5}$$

where $\boldsymbol{V} = (\boldsymbol{v}_1, \boldsymbol{v}_2, ..., \boldsymbol{v}_n)$ is a matrix, normalised such that $\boldsymbol{V}^T\boldsymbol{M}_{11}\boldsymbol{V} = \boldsymbol{I}$, of the first n mode shapes and $\boldsymbol{z}$ the vector of modal amplitudes. Eq. 2 can now be written as:

$$\ddot{\boldsymbol{z}} + \boldsymbol{V}^T\boldsymbol{C}_{11}(\dot{\Phi})\boldsymbol{V}\dot{\boldsymbol{z}} + \boldsymbol{V}^T\boldsymbol{D}_{11}\boldsymbol{V}\dot{\boldsymbol{z}} + \boldsymbol{V}^T\boldsymbol{K}_{11}\boldsymbol{V}\boldsymbol{z} + \boldsymbol{V}^T\boldsymbol{N}_{11}(\dot{\Phi}^2)\boldsymbol{V}\boldsymbol{z} = \boldsymbol{V}^T\boldsymbol{f} + \boldsymbol{V}^T\boldsymbol{f}_{dis} \tag{6}$$

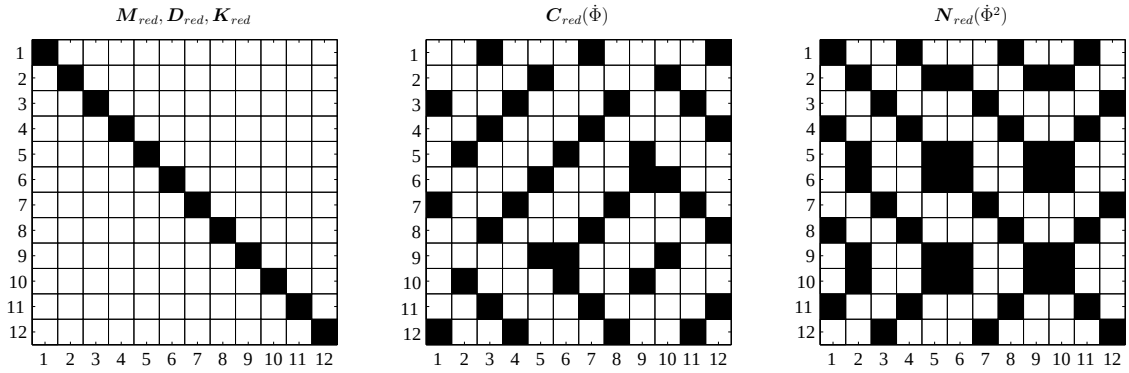

(a) Mass, Damping and Stiffness matrix (b) Velocity sensitivity matrix (c) Dynamic stiffness matrix

Figure 3: Reduced system matrices with the first 12 mode shapes, describing the coupling between the mode shapes as function of the mass-flow $\dot{\Phi}$

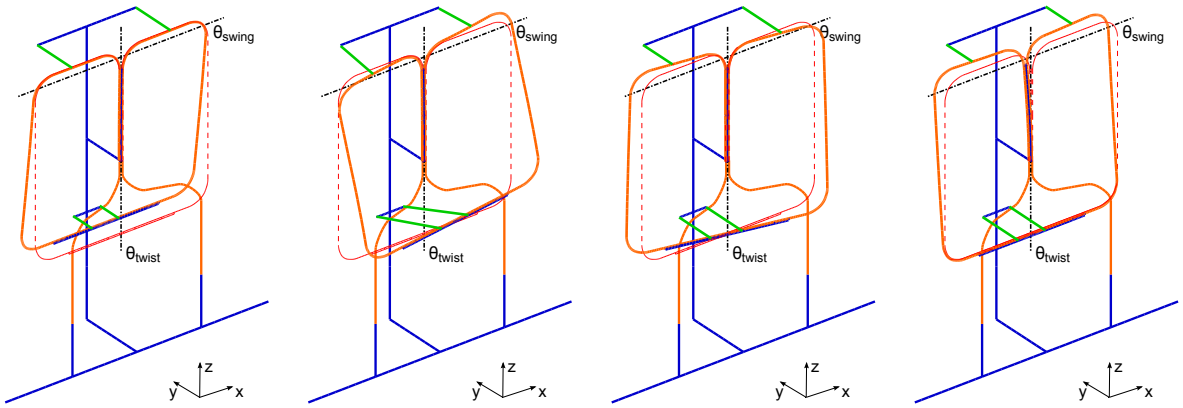

(a) Mode 1 - First Coriolis mode - 42 Hz (b) Mode 2 - Plane mode - 62 Hz (c) Mode 3 - Actuation mode - 88 Hz (d) Mode 4 - Second Coriolis mode - 210 Hz

Figure 4: CMFM mode shapes with their corresponding natural frequencies, when the tube is filled with air

Using the multi-body package SPACAR [4] the system matrices with respect to the element deformations and imposed floor movements of the model are derived.

The reduced matrices of Eq. 6 (e.g. $\boldsymbol{K}_{red} = \boldsymbol{V}^T \boldsymbol{K}_{11} \boldsymbol{V}$) with the first 12 modes are derived for the model described above. In Figure 3 the non-zero elements of the matrices are depicted. The modal mass and stiffness matrix are diagonal by the definition of the modal coordinates. The modal damping matrix is also diagonal since proportional damping is assumed. The velocity sensitive matrix and the dynamic stiffness matrix are dependent on the mass-flow and describe the coupling between the modes. Those matrices are zero in the case of a zero mass-flow $\dot{\Phi} = 0$.

In Figure 4 the first four mode shapes of the tube-window are depicted. The second mode is called an in-plane mode, because it has no displacement in the direction of the sensors. The third mode is the actuation mode of this instrument. When the third mode is actuated and there is a mass-flow also modes 1,4,8 and 11 are actuated (see Figure 3(b)). Therefore these modes are called Coriolis modes, because the coupling is due to the Coriolis effect. In Figure 5 the flow induced mode is depicted, which is a combination of the mode shapes 1, 3 and 4 (see Figure 4), moving at the natural frequency belonging to mode 3.

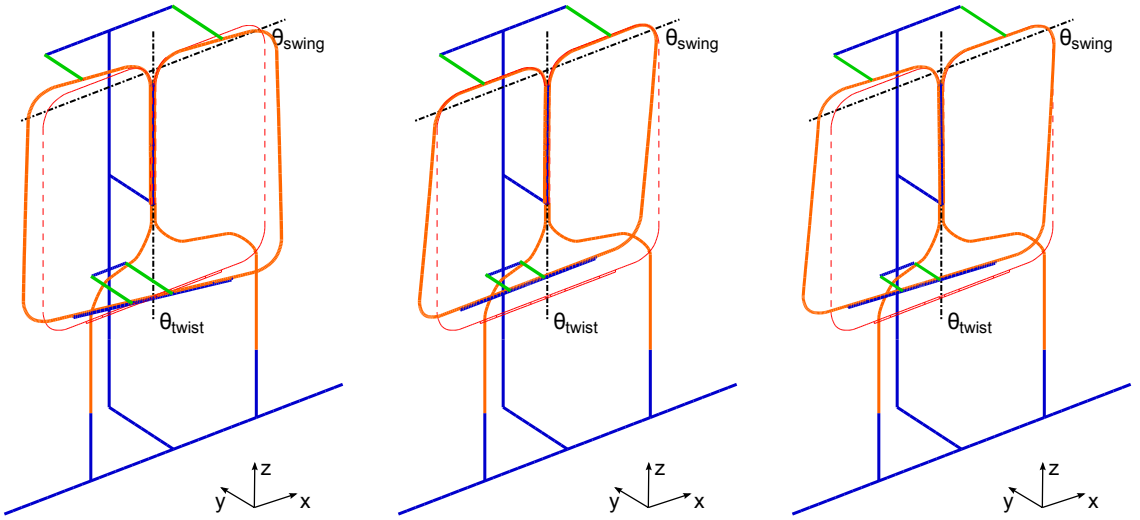

(a) Actuation mode - 88 Hz - $t = \frac{\pi}{2\omega_3} + \frac{2k\pi}{\omega_3}, k = 0, 1, 2, ..$

(b) Flow induced mode - 88 Hz - $t = 0 + \frac{2k\pi}{\omega_3}, k = 0, 1, 2, ..$

(c) Combination - 88 Hz - $t = \frac{\pi}{3\omega_3} + \frac{2k\pi}{\omega_3}, k = 0, 1, 2, ..$

Figure 5: The mode shape of the actuated instrument is a combination of the actuation mode (Figure 4(c)) and mass-flow $\dot{\Phi}$ induced Coriolis modes (Figure 4(a) and 4(d)), whereby the flow-induced mode (b) is 90° out of phase with the actuation mode (a). The sensors s_1 and s_2 measure the movement of the tube-window: $s_i = A_i \sin(\omega_3 t + \phi_i)$ with ω_3 the natural frequency belonging to mode 3.

2.2 Actuation

The flexible tube-window is actuated to have an oscillation around the θ_{twist}-axis (see Figure 2), therefore in the model a moment is applied by two forces between the tube and the casing. In model terms the actuator input is equal to:

$$\boldsymbol{f} = \frac{1}{r_M}(\boldsymbol{\Gamma}_{act1} - \boldsymbol{\Gamma}_{act2})M_{act} \tag{7}$$

where $\boldsymbol{\Gamma}_{act1}$ is a vector with the elongation of the actuator element with respect to the coordinates of the model, r_M the distance between the two actuator elements and M_{act} the actuator moment input.

2.3 Sensing

The movement of the tube-window is measured by two sensors, s_1 and s_2. In Figure 5(a) the actuation mode is shown, an oscillation around the θ_{twist}-axis. The actuation displacement is the differential-mode signal of the sensor signals. Accordingly the Coriolis displacement, due to an oscillation around the θ_{swing}-axis (see Figure 5(b)), is the common-mode signal of the sensor signals. In model terms the actuation and Coriolis displacement are equal to:

$$y_{act} = \frac{1}{2}(\boldsymbol{\Gamma}_{s_1} - \boldsymbol{\Gamma}_{s_2})\boldsymbol{V}\boldsymbol{z} \tag{8}$$

$$y_{cor} = \frac{1}{2}(\boldsymbol{\Gamma}_{s_1} + \boldsymbol{\Gamma}_{s_2})\boldsymbol{V}\boldsymbol{z} \tag{9}$$

where $\boldsymbol{\Gamma}_s$ is a vector with the elongation of the sensor elements with respect to the coordinates of the model.

2.4 State space representation

Combining the equations of the previous sections, a state space representation of the CMFM with a state vector $\boldsymbol{x} = \begin{bmatrix}\boldsymbol{z} & \dot{\boldsymbol{z}}\end{bmatrix}^T$, input vector $\boldsymbol{u} = \begin{bmatrix}M_{act} & \boldsymbol{a}_0\end{bmatrix}^T$ and output vector $\boldsymbol{y} = \begin{bmatrix}y_{act} & y_{cor}\end{bmatrix}^T$ is derived:

$$\begin{aligned}\dot{\boldsymbol{x}} &= \begin{bmatrix}\boldsymbol{0} & \boldsymbol{I} \\ -\boldsymbol{V}^T\boldsymbol{K}\boldsymbol{V} - \boldsymbol{V}^T\boldsymbol{N}(\dot{\Phi}^2)\boldsymbol{V} & -\boldsymbol{V}^T\boldsymbol{C}(\dot{\Phi})\boldsymbol{V} - \boldsymbol{V}^T\boldsymbol{D}\boldsymbol{V}\end{bmatrix}\boldsymbol{x} + \\ &\quad \begin{bmatrix}\boldsymbol{0} & \boldsymbol{0} \\ \boldsymbol{V}^T\frac{1}{r_M}(\boldsymbol{\Gamma}_{act1} - \boldsymbol{\Gamma}_{act2}) & -\boldsymbol{V}^T\boldsymbol{M}_{12}\end{bmatrix}\boldsymbol{u} \\ \boldsymbol{y} &= \begin{bmatrix}\frac{1}{2}(\boldsymbol{\Gamma}_{s_1} - \boldsymbol{\Gamma}_{s_2})\boldsymbol{V} & \boldsymbol{0} \\ \frac{1}{2}(\boldsymbol{\Gamma}_{s_1} + \boldsymbol{\Gamma}_{s_2})\boldsymbol{V} & \boldsymbol{0}\end{bmatrix}\boldsymbol{x} + \begin{bmatrix}\boldsymbol{0}\end{bmatrix}\boldsymbol{u}\end{aligned} \tag{10}$$

where y_{act} is due to an actuation M_{act} and y_{cor} due to a mass-flow $\dot{\Phi}$ or a floor disturbance $\boldsymbol{a}_0$.

In this section a state-space representation of a CMFM is derived, which can be used to investigate the response of the Coriolis displacement of a CMFM to an actuation moment and floor vibrations.

3 RESULTS

In this section the modelled influence of floor vibrations on a mass-flow measurement is validated. First, the measurement value and sensitivity of a CMFM is presented. Secondly, the frequency dependent influence of floor vibrations is presented and validated with an experimental sweep. Thirdly the time dependent influence of floor vibrations on the measurement value is compared with the estimated value from the model.

3.1 Measurement value

The tube-window is excited in its third eigenmode and a mass-flow induces a flow induced vibration mode due to the Coriolis effect. This vibration mode occurs 90° out of phase with the actuation mode. When a fluid flow is affecting the vibration mode of the tube-window, the phase-difference between the sensor signals s_1 and s_2 is not 180° anymore, but is dependent on the mass-flow. The phase-difference between the two sensor signals is expressed as:

$$\Delta\phi \approx \arctan(\Delta\phi) = 2\frac{s_1 + s_2}{s_1 - s_2} = 2\frac{y_{cor}}{y_{act}} \tag{11}$$

where the differential-mode $s_1 - s_2$ is named the actuation displacement y_{act} and the common-mode $s_1 + s_2$ the Coriolis displacement y_{cor}. The approximation is valid for small flows, because then the Coriolis displacement is small compared to the actuation displacement.

When the model, undisturbed by floor vibrations, is actuated with a certain moment M_{act}, an actuation displacement y_{act} and a Coriolis displacement y_{cor}, proportional to the mass-flow $\dot{\Phi}_0$ is obtained. This results in a modelled measurement sensitivity, which is the phase difference (Eq. 11) per unit mass-flow:

$$S := \frac{\Delta\phi(\omega = \omega_3)_{\boldsymbol{a}_0=0, y_{act}\neq 0, \dot{\Phi}=\dot{\Phi}_0}}{\dot{\Phi}_0}\left[\frac{rad\cdot s}{kg}\right] \tag{12}$$

where ω_3 is the natural frequency belonging to mode 3, the actuation mode. The mass-flow can be determined from the measured phase difference and the measurement sensitivity. The measurement sensitivity S is instrument dependent and is not given for the used instrument (Figure 1), but the phase difference $\Delta\phi$ is also a valid measure for the mass-flow.

3.2 Frequency dependent influence floor vibrations

Eq. 11 shows that a Coriolis displacement results in a mass-flow measurement. As explained before, this displacement is not only occurring due to a mass-flow, but also due to floor vibrations, resulting in a measured mass-flow:

$$\Delta\phi_{measured} = 2\frac{y_{cor}}{y_{act}} = \frac{2}{y_{act}}(T_{y_{cor,\dot{\Phi}}}\dot{\Phi} + \boldsymbol{T}_{y_{cor,a_0}}\boldsymbol{a}_0) \tag{13}$$

where $T_{y_{cor,\dot{\Phi}}}$ and $\boldsymbol{T}_{y_{cor,a_0}}$ are the Coriolis displacement contribution due to respectively the actuation and casing movements. Using the state space model (Eq. 10) the influence of floor vibrations is:

$$\boldsymbol{T}_{\Delta\phi,a_0} = \frac{2}{y_{act}}\boldsymbol{T}_{y_{cor},\boldsymbol{a}_0} \tag{14}$$

where the actuation mode is controlled, resulting in a constant y_{act}.

The transmissibility from a floor displacement in the dominant direction a_y to Coriolis displacement and thus a mass-flow error is depicted in Figure 6. The dominant disturbance is a translation disturbance of the casing in the direction of the sensors and actuating directly on the Coriolis modes, see Figure 4(a) and 4(d). Resonance frequencies are visible at the Coriolis modes (42, 210 Hz). The frequency axis shows the frequency value of the disturbance a_y.

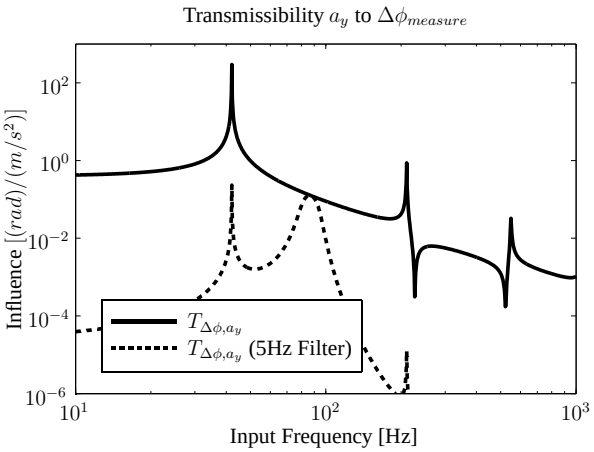

Figure 6: Transmissibility of floor disturbances in the dominant direction a_y to a mass-flow measurement (Eq. 14), with and without the phase demodulation including a 5Hz low pass filter.

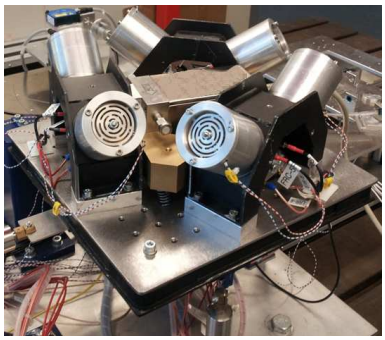

Figure 7: Shaker setup - The CMFM (Figure 1) is mounted on a Stewart platform. Voice coil actuators are used to apply forces on the low frequent (25Hz) suspended platform and accelerometers are used to measure the platform vibrations $\boldsymbol{a}_0$.

In section 2.1 is mentioned that the tube-window is actuated to oscillate in a mode shape with the natural frequency ω_3, where the mode shape depends on the mass-flow. To calculate the phase difference between the sensors s_1 and s_2 a technique, called phase demodulation, is used. The phase demodulation effectively results in a frequency shift and is implemented by multiplying the sensor data with an oscillating reference signal with the actuation frequency ω_3 and subsequently low pass filtering. In the frequency domain, this is similar to a bandpass filter around frequency ω_3. The frequency of measured mass-flow is the difference between the input frequency and the actuation frequency.

Due to the phase demodulation, only disturbances around the actuation frequency have an influence on the measurement value, as shown by the transmissibility including a 5 Hz low

pass filter in Figure 6. The result is that a disturbance with a frequency close to the actuation frequency has a direct impact on a mass-flow reading.

An experiment is performed with a shaker (see Figure 7) to apply a disturbance sweep with an increasing frequency (see Eq. 15), meanwhile the mass-flow measurement and instrument casing accelerations are recorded.

$$f_{sweep} = f_1 \left(\frac{f_2}{f_1} \right)^{\frac{t}{T}}, f_1 = 10Hz, f_2 = 200Hz, T = 600s \tag{15}$$

The results of two sweep experiments are given in Figure 8. The mass-flow measurement is divided by the measured casing acceleration for each frequency of the sweep to calculate the frequency dependent influence of floor vibrations on the flow measurement. Around the actuation mode (88Hz) the result of sweep fits the model and a peak is visible around the Coriolis mode (42 Hz). In the low and high frequency region the influence cannot be measured, due to the low-pass filter and the noise level of the measurement value.

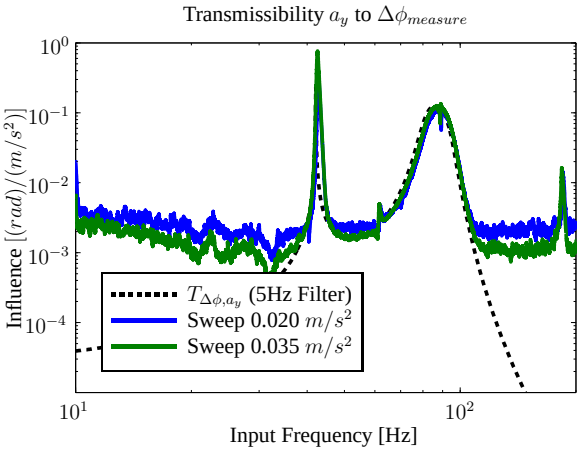

Figure 8: Transmissibility of floor disturbances in the dominant direction a_y to a mass-flow measurement, validated by two experimental sweeps.

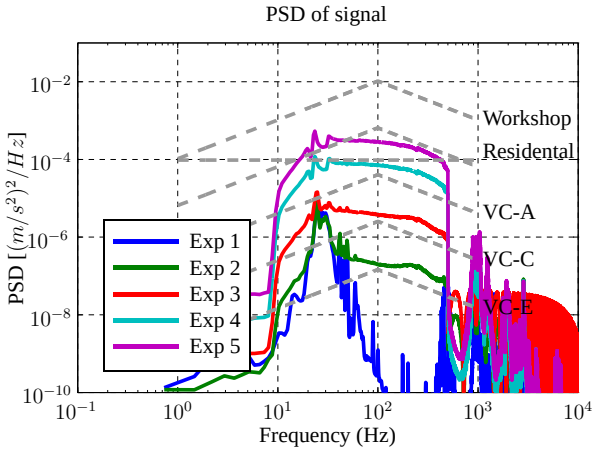

Figure 9: Measured floor vibration PSDs $\mathbf{\Phi}_{a_y}$ of 5 experiments compared to VC-curves to show the magnitude of the disturbance. The applied disturbances are relatively large in comparison to real floor spectra.

3.3 Time dependent influence floor vibrations

The floor vibration can be a broadband disturbance, but the output is a single measurement value, the mass-flow measurement. The cumulative influence is investigated by looking to the cumulative mean square response over the whole frequency range ν, which is given by:

$$\sigma^2_{\Delta\phi} = \int_0^\infty |\boldsymbol{T}_{\Delta\phi,a_y}(\nu)|^2 \mathbf{\Phi}_{a_y}(\nu)\, \mathrm{d}\nu \tag{16}$$

where $\mathbf{\Phi}_{a_y}$ is the Power Spectral Density (PSD) function of the disturbance and $\boldsymbol{T}_{\Delta\phi,a_y}$ the modelled transmissibility of floor vibrations resulting in a mass-flow error, as depicted in Figure 8. In Section 3.2 the function $\boldsymbol{T}_{\Delta\phi,a_y}$ is explained and validated for the investigated instrument. PSDs of several experiments, with a multi sine disturbance between 10 and 500Hz, are given in Figure 9, including the Vibration Criterion (VC) curves [10], which are extended with a decreasing trend above 100Hz. The disturbances are relatively large in comparison to real floor

Experiment	Disturbance RMS $[m/s^2]$	Measurement value instrument FlowPlot RMS $[mrad]$	Model estimation $\sigma_{\Delta\phi}$ (Eq. 16) $[mrad]$
1	0.0072	0.041	0.022
2	0.0113	0.189	0.194
3	0.0377	0.756	0.826
4	0.1492	3.184	3.525
5	0.2977	7.797	7.024

Table 1: Mass flow error due to applied disturbance (Figure 9). The disturbance RMS is the cumulative RMS value by integrating the disturbance PSD.

spectra to magnify the effect on the flow error. The VC-curves are meant as upper bounds for the peaks in the floor vibration spectrum.

Using this data, $\sigma_{\Delta\phi}$ is calculated. The results are given in Table 1. For experiment 2-4 the estimation shows the same trend as the measured value. In experiment 5 the disturbance is so large that non-linear effects are occurring due to the limited sensor range, resulting in a higher measurement value. In the first experiment the measured value is comparable to the noise floor of the measurement and the estimation shows that the noise floor is not due to external vibrations.

To minimise the error the disturbance $\mathbf{\Phi}_{a_y}$ should be minimal, but in many applications stringent requirements on the surroundings are not possible, so $\boldsymbol{T}_{\Delta\phi,\boldsymbol{a}_0}$ should be minimal, implying a good filter algorithm and mechanical design of the instrument, which will be subject of future research.

4 CONCLUSIONS

In this study a model of a CMFM is derived to determine the influence of floor vibrations on the mass-flow measurement. In an experiment predefined vibrations are applied on the casing of the CMFM and the error is determined. The results correspond with the obtained model results.

The result is an improvement on the work of Cheesewright [3], not only the frequencies are shown where the CMFM is sensitive for floor vibrations, but also a quantitative estimation of the expected mass-flow error is given, based on the modelled transmissibility function.

The agreement between model and measurements implies firstly that the influence of any floor vibration spectrum on the flow error, with some limitations due to linearity of the model, can be estimated. Thereby, the suitability of a certain location for the placement of a CMFM can be determined. Secondly, the insight in the relation between vibration spectra and the flow error, the transmissibility, can be used to compare the performance of different CMFM designs and to optimise the performance by shaping their respective transfer functions.

ACKNOWLEDGEMENTS

This research was financed by the support of the Pieken in de Delta Programme of the Dutch Ministry of Economic Affairs. The authors would like to thank the industrial partner Bronkhorst High-Tech for many fruitful discussions.

REFERENCES

[1] M. Anklin, W. Drahm, and A. Rieder, "Coriolis mass flowmeters: Overview of the current state of the art and latest research," *Flow Measurement and Instrumentation*, vol. 17, no. 6, pp. 317 – 323, 2006.

[2] C. Clark and R. Cheesewright, "The influence upon coriolis mass flow meters of external vibrations at selected frequencies," *Flow Measurement and Instrumentation*, vol. 14, no. 1-2, pp. 33 – 42, 2003.

[3] R. Cheesewright, A. Belhadj, and C. Clark, "Effect of mechanical vibrations on coriolis mass flow meters," *Journal of Dynamic Systems, Measurement, and Control*, vol. 125, no. 1, pp. 103–113, 2003.

[4] J. B. Jonker, "A finite element dynamic analysis of spatial mechanisms with flexible links," *Computer Methods in Applied Mechanics and Engineering*, vol. 76, no. 1, pp. 17 – 40, 1989.

[5] J. B. Jonker, R. G. K. M. Aarts, and J. van Dijk, "A linearized input–output representation of flexible multibody systems for control synthesis," *Multibody System Dynamics*, vol. 21, pp. 99–122, 2009.

[6] J. P. Meijaard and W. B. J. Hakvoort, "Modelling of fluid-conveying flexible pipes in multibody systems," in *7th EUROMECH Solid Mechanics Conference*. University of Twente, Enschede, The Netherlands, 2009.

[7] W. B. J. Hakvoort, J. P. Meijaard, R. G. K. M. Aarts, J. B. Jonker, and J. M. Zwikker, "Modeling a coriolis mass flow meter for shape optimization," in *The 1st Joint International Conference on Multibody System Dynamics*. University of Twente, Enschede, The Netherlands, 2010.

[8] A. Mehendale, J. C. Lötters, and J. M. Zwikker, "Mass flowmeter of the coriolis type¨ and ¨Coriolis mass flow meter using contactless excitation and detection," EU Patent EP 1 719 982 and EP 1 719 983, 2006.

[9] A. Mehendale, "Coriolis mass flow rate meters for low flows," Ph.D. dissertation, University of Twente, Enschede, October 2008.

[10] C. G. Gordon, "Generic vibration criteria for vibration-sensitive equipment," in *Society of Photo-Optical Instrumentation Engineers (SPIE) Conference Series*, ser. Presented at the Society of Photo-Optical Instrumentation Engineers (SPIE) Conference, C. G. Gordon, Ed., vol. 1619, Feb. 1992, pp. 71–85.